Biodegradable Elastomers with Antioxidant and Retinoid-like Properties

Robert van Lith[a‡], *Xuesong Wang*[a‡] *and Guillermo Ameer*[a,b,c,d,e*]

[a]Biomedical Engineering Department, Northwestern University, Evanston, IL 60208, USA

[b]Department of Surgery, Feinberg School of Medicine, Chicago, IL 60611, USA

[c]Chemistry of Life Processes Institute, Northwestern University, Evanston, IL 60208, USA

[d]Simpson Querrey Institute for BioNanotechnology in Medicine, Northwestern University, Chicago, IL 60611, USA

[e]International Institute for Nanotechnology, Northwestern University, Evanston, IL 60208, USA

Supporting Information

S1. Free radical scavenging of free atRA

Free radical scavenging activity of atRA was measured using a (1, 1-diphenyl-2-picrylhydrazyl) (DPPH) free radical assay. To 1 mL of DPPH (200 μM in ethanol) free atRA was added and samples were incubated at 37°C. At predetermined time points, supernatants were taken. DPPH is a stable free radical in EtOH with a deep violet color. Upon radical scavenging activity, by the antioxidant material, a color change to pale yellow will be observed. This discoloration was monitored by measuring the absorbance change at 517 nm using a micro plate

reader. Antioxidant activity in terms of scavenging DPPH free radicals was calculated as scavenging percentage of DPPH radical by measuring the decrease of absorbance compared to non-reacted solution and fully-reacted solution. All measurements were performed in triplicate. Free atRA at concentrations of 0.2 and 0.8 mg/mL could dose-dependently scavenge DPPH radicals (**Fig. S1A**).

S2. Iron chelation of free atRA

The extent of metal chelation by free atRA was measured using a ferrous iron chelation assay. To 200 μL of $FeCl_2 \cdot 4\ H_2O$ solution (1 mM in MQ) free atRA was added and samples were incubated at 37°C. Supernatants were collected and reacted with 5 mM of ferrozine iron reagent solution at a volume ratio of 5: 1. Chelating activity is indicated by inhibition of the purple Fe^{2+}-ferrozine complex formation, as Fe^{2+} chelated can not react with ferrozine. The inhibition can be monitored as a decrease in absorbance at 534 nm. Chelation is calculated as a percentage of decreased absorbance compared to a no-chelation control. All measurements were taken in triplicate. Free atRA showed an initial mild chelation of iron, but over tie this effect disappeared, indicating weak chelation with labile coordination bonds (**Fig. S1B**).

S3. Lipid peroxidation inhibition by free atRA

The lipid peroxidation inhibition capacity of free atRA was determined by performing a β-carotene bleaching assay according to a previously published protocol (see main text). Briefly, β-carotene (4 mg), linoleic acid (0.5 mL) and tween 40 (4 g) were mixed, dissolved in chloroform (20 mL) and vigorously shaken. This was followed by chloroform evaporation using rotary evaporation, resulting in viscous BC reagent. Britton buffer (pH 6.5, pre-warmed to 45°C) was

added (30 mL to 1 mL BC reagent) to form a clear suspension. Free atRA was added to 1 mL of the suspension and samples were incubated at 45°C. Supernatants were collected at various time points and the absorbance monitored at 470 nm. Spontaneous peroxidation of linoleic acid at 45°C causes β-carotene discoloration and inhibition of linoleic acid peroxidation can be detected as a reduction in absorbance decrease. All measurements were performed in triplicate. Free atRA could dose-dependently inhibit lipid peroxidation (**Fig. S1**).

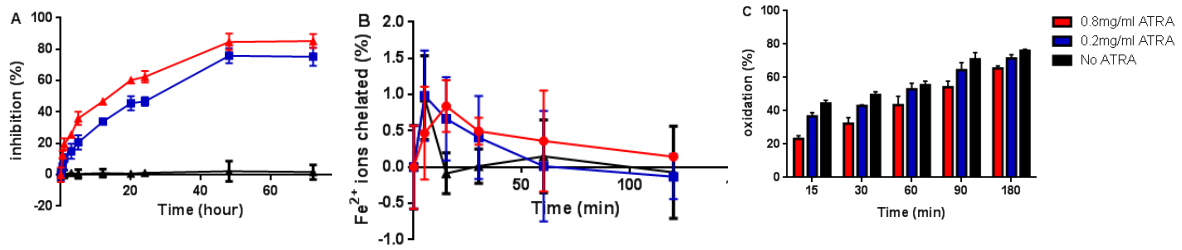

Figure S1: A) DPPH assay shows dose-dependent free radical inhibition by free atRA. B) Free atRA is not capable of stable iron ion chelation. C) Free atRA dose-dependently inhibits lipid peroxidation. N =3, Mean ± SD. *p < 0.05 **p < 0.01, ***p < 0.001.

S4. Mechanical properties

Tensile testing on POC, POCR-4 and POCR-16 was performed according to American Society for Testing and Materials (ASTM) 412A on an Instron 5544 equipped with 500-N load cell (Instron, Norwood, MA). Briefly, dumbbell-shaped samples were pulled to failure at a rate of 500 mm/min. Young's modulus, ultimate tensile strength and elongation at break were obtained from stress–strain curves. No differences were found between polymers in Young's moduli or ultimate tensile strengths, while the elongation at break was slighty increased in the POCR-4 polymers compared to POC, yet no other difference were observed (**Fig. S2A**). The pre-testing

dimensions of polymer strips were recovered after tensile testing (**Fig. S2B**). Together, these results confirm that atRA incorporation does not significantly change mechanical properties, while POC and POCR polymers are elastomeric.

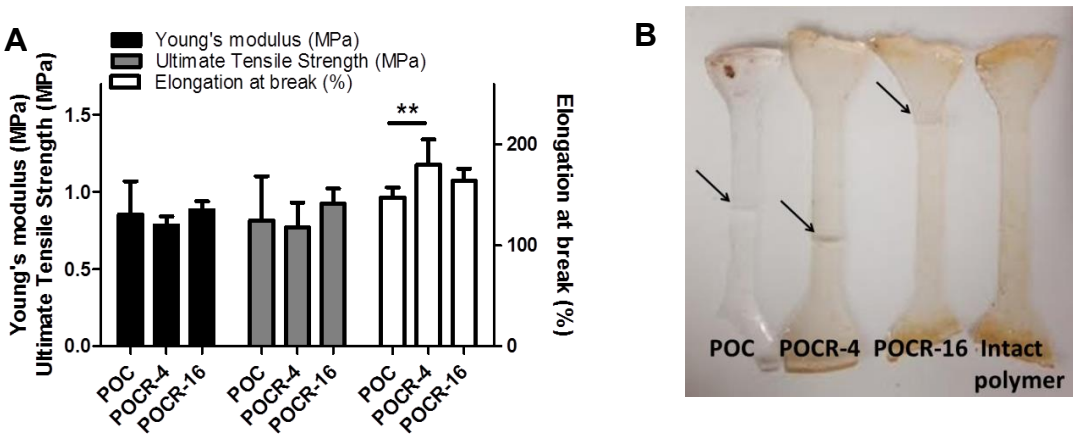

Figure S2: A) Tensile testing of POC and POCR shows limited effect of atRA incorporation on Young's modulus, ultimate tensile strength and elongation at break. B) Digital photographs of POC and POCR polymers after tensile testing indicates elastomeric properties with strips returning to original length after breaking at approximately 150-180% elongation. Arrows indicate point of rupture. N =3, Mean ± SD. *$p < 0.05$ **$p < 0.01$, ***$p < 0.001$.

S5. Fourier transformed infrared spectroscopy

Fourier Transform Infrared (FTIR) spectroscopy was used in attenuated total reflection mode on final post-polymerized polymer films POC and POCR-16 (5 days at 60°C). Spectra were recorded by accumulation of 64 scans, with a resolution of 8 cm^{-1}. Contrary to POCR-16 after only 2 days of post-polymerization (see main text), no remaining peak around 1690 cm^{-1} could be observed, but atRA C=C characteristic peaks were present (**Fig. S3A**).

S6. H NMR

^{H}NMR was performed on the viscous POCR-16 polymer product in DMSO-d_6 after 2 days of post-polymerization at 60°C to determine atRA incorporation. No –COO**H** peak specific to atRA at 12.0 ppm could be observed, indicating esterification of atRA to POC (**Fig. S3B**).

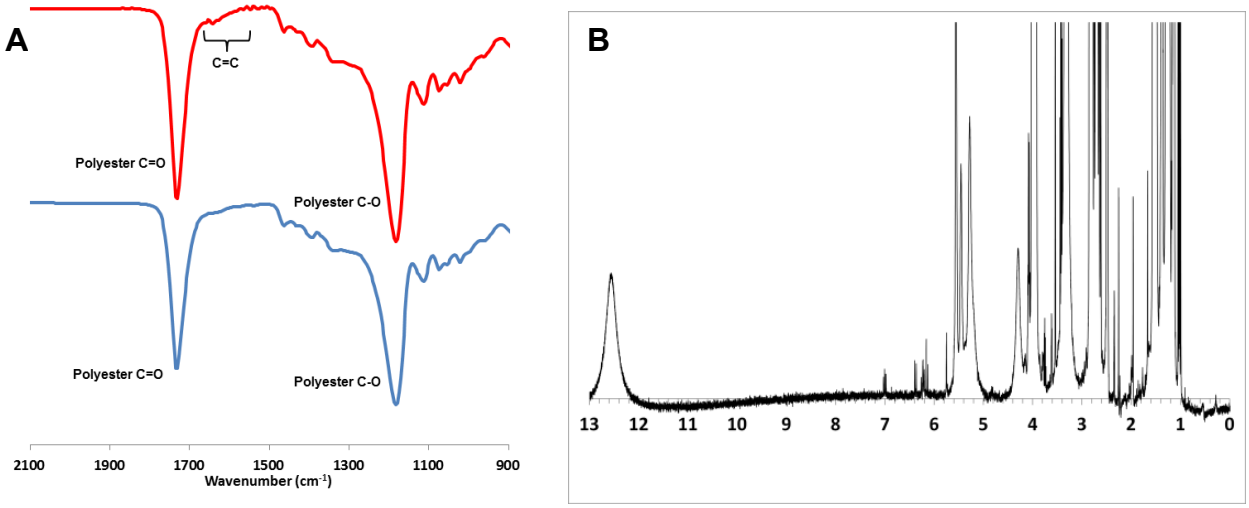

Figure S3: A) FTIR spectra of poly(octamethylene-citrate) (POC) and poly(octamethylene-citrate-co-retinate)(POCR-16) using attenuated total reflectance FTIR on fully post-polymerized polymer films. B) ^{H}NMR close-up of POCR-16 indicating absence of free atRA-characteristic peak at 12.0 ppm.

S7. Cell morphology

Cell morphology of HUVECs and HASMCs was assessed after 3 days of culture on TCP, POC, POCR-4 and POCR-8 surfaces using light microscopy on a TE2000 microscope (Nikon) (**Figure S4**). HUVECs could attach and showed typical endothelial rounded cobblestone morphology on

all surfaces, although on all polymer surfaces some cells detached more easily compared to TCP. HASMCs, on the other hand, showed excellent spreading and morphology retention on all surfaces.

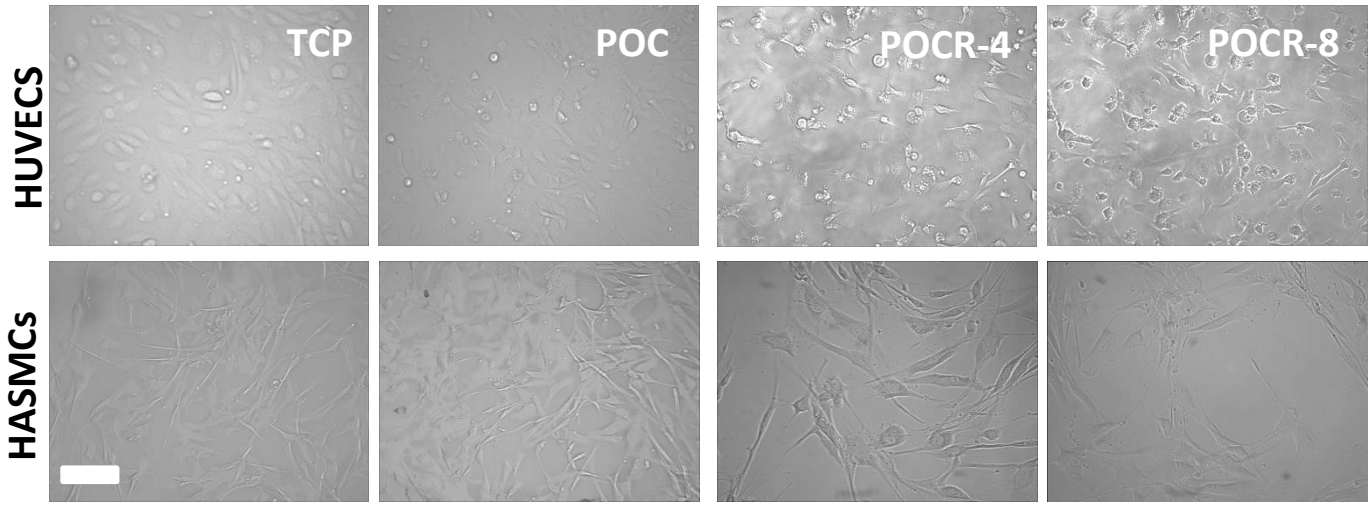

Figure S4: Morphology of human umbilical vein endothelial cells (HUVECs) and human aortic smooth muscle cells (HASMCs) on tissue culture plastic (TCP), poly(1,8-octamethylene citrate)(POC) and Poly(1,8-octamethylene citrate-co-retinate) (POCR). POCR-4 and POCR-8 indicate atRA loading of 4 and 8 µg/mg polymer, respectively. Scale bar=100 µm.